

The mechanism research for the surface plasmon-catalysed reaction of the mercapto group substituted benzoic acid.

Received: July 16, 2017,
Accepted: September 5, 2017

Jiyu Wang^a, Jing Wang^b, Caiqing Ma^b, Meixia Zhang^a, Yong Ding^a, Peng Song^{a,*} and Fengcai Ma^{a,*}

DOI: 10.4208/jams.071617.090517a

<http://www.global-sci.org/jams/>

Abstract. In this study, we experimentally investigated the substituent effect on benzoic acid where the mercapto group was located in different positions, namely as 2-mercaptobenzoic acid (2-MBA), 3-mercaptobenzoic acid (3-MBA) and 4-mercaptobenzoic acid (4-MBA). The substituent effect was found to have an influence on the surface plasmon-catalysed reaction on the surface of the Ag₄ atoms in the reaction of MBA with silver sol. In addition to the direct evidence from the surface-enhanced Raman scattering (SERS), the chemical enhancement mechanism for the generation of the MBA–Ag complex is presented. In contrast with the normal Raman scattering (NRS) spectra, new signals appeared in the SERS spectra of 2-MBA, 3-MBA and 4-MBA under the theoretical and experimental conditions. On investigation of the SERS spectra, the characteristic peaks of the C≡C bond have been demonstrated. The structural, atomic and chemical bond properties of the three types of MBAs indicate that the S atom of the mercapto group in the MBA molecules is the position site that attaches to the silver substrate through the bond of S···Ag, and under laser irradiation, “hot electrons” are generated between the surface of MBA and Ag₄ atoms. With the effect of “hot electrons”, the –COOH bond of the MBA molecules is broken, and then the two single carboxylate MBA molecules become dimerized thiophenol acetylene (TPA). To briefly consider the substituent effect, the SERS spectra of these three types of MBAs were specifically studied for the enhancement of the Raman signal intensity with a variational tendency evident. Therefore, the conclusion was reached that the substituent effect plays a vital role in the surface plasmon-catalysed reaction, where the changing of the surface-enhanced Raman intensity was demonstrated.

Key words: Surface plasmon-catalysed reaction, MBA, thiophenol acetylene (TPA), normal Raman scattering (NRS) spectra, surface-enhanced Raman scattering (SERS) spectra, hot electron, substituent effect.

1. Introduction

In addition to identifying types of material, Raman spectroscopy is mainly used to measure molecular vibration frequencies and quantitatively analyse the phenomena of intermolecular and intramolecular forces [1,2]. Thus, molecular symmetry, geometric structure formation and how atoms are arranged in molecules can be inferred using Raman spectroscopy. Since 1974, scientists have found that surface-enhanced Raman scattering (SERS) technology [3–5] (based on its high sensitivity, little interference by water, formal research of interface effect, and so on) has played a powerful role in interface features and ultrathin membrane material research; it has thrived both in theory and experiment due to its extensive applications in fingerprint detection, even at the single molecule level [6–9]. SERS is the most extensive spatial location technique involving the adsorption process at solid or liquid interfaces because of its simplicity and ability to recognize the material structures rapidly, along with its ability

to detect different types of supramolecular architectures as well as its ability to investigate distinct functional group adsorption phenomena [10–12]. As a potentially comprehensive application, many investigations have been presented on the mechanism of SERS [13,14].

The self-assembled monolayer, with organic small molecules that contain the mercapto group on the surface of the metal film, has been widely used in embellishing electrodes, biological sensors and other research fields [15–17]. Furthermore, thiol molecules along with some other molecules with specific functional groups were usually regarded as the superior substance for SERS recognition, as the formation of Au-MBA@SiO₂ nanoparticles was achieved on the basis of Stöber's method by the hydrolysis of TEOS. The thiol compounds with containing aromatic rings are noteworthy, especially in recent years [6].

Miriam C. Rodríguez González et al. conducted STM that the Au(111) surface after 2-MBA adsorption shows atomically smooth terraces separated by steps of monatomic height, without any evidence of vacancy island formation, through the detection of 2-MBA and 4-MBA that adsorbed on the surface of Au(111), showing atomically smooth terraces separated by steps of monatomic height [18]. These compounds revealed the favourable adsorption on the noble metal nanoclusters with rigid structure stability, and the monolayer film also had

^a Department of Physics, Liaoning University, Shenyang 110036, P. R. China.
songpeng@lnu.edu.cn

^b Department of Chemistry, Liaoning University, Shenyang 110036, P. R. China.

^c Institute of Theoretical Simulation Chemistry, Academy of Fundamental and Interdisciplinary Sciences, Harbin Institute of Technology, Harbin 150080, China

^d Normal College, Shenyang University, Shenyang 110044, China

excellent electrical conductivity [19–21], showing potential application in the design of molecule-conducting wire [22].

At first, in the process of vigorous study using SERS, we explored the material properties just through its signal increasing by the adsorption between the substance and the metal surface, and then we explored an intensive chemical reaction arising spontaneously based on the SERS mechanism. Thus, in this study we used SERS as a starting point, and discuss the surface plasmon-catalysed reaction occurring for three types of MBA that adsorbed on the silver surface.

Surface plasmons (SPs) are collective electron oscillations confined evanescently along the interface between a conductor and a dielectric [23,24]. It is often assumed that the material adsorbed on the silver surface, and the silver atoms exist under this relationship. It is well known that the electrons on the surface of a metal can absorb a certain energy of an electric field (such as photons, etc.), then they would be excited, and these electrons are called “hot electrons” in the excited states [25–28]. Under the effects of surface plasmons and “hot electrons”, the surface plasmon-catalysed reaction would take place.

In physical chemistry, the substituent effect has tremendous significance in understanding and quantitatively analysing the performance activity relations of molecular structures [28]. In this article, we use the centrifuge to mixed mercaptobenzoic acid (2-MBA, 3-MBA and 4-MBA) 10^{-5} mol/L sample solution and silver sol solution sufficiently to obtained the centrifugal sedimentation of the mixture. Herein, comparison of SERS signals of the MBAs indicated a changing tendency, with a remarkable discovery of the substituent effect playing a crucial role in the surface plasmon-catalysed reaction and demonstrated in detail.

2. Experimental section

In order to measure SERS, the silver sol was prepared under high vacuum using a vacuum electron beam evaporator. Silver sol was generated by a silver nitrate and trisodium citrate reduction reaction. As follows, silver nitrate solution was heated until boiling, and then the silver nitrate solution was poured into trisodium citrate (10 mL). The mixture was heated for an hour with stirring, and then cooling the heated mixture. In our experiment the anhydrous ethanol was purchased from Tianjin Yongda Chemical Reagent Co., Ltd. (China). The three types of MBA solid powder samples were 2-mercaptobenzoic acid (2-MBA), 3-mercaptobenzoic acid (3-MBA) and 4-mercaptobenzoic acid (4-MBA) that obtained from AR, Aladdin Reagent Co., Ltd. Then these MBA powder samples were mixed with anhydrous ethanol to gain solution that the concentrations of 10^{-5} mol/L. Next, the solution of the 2-MBA was mixed in silver sol (with the proportion of 1 to 5) that add the silver sol of 5ml and 2-MBA solution of 1ml. Finally, the mixture was placed into the ultracentrifuge with centrifuging 8000 rad/min for 15 mins. After this process, the supernatant and sediment were separated. The sediment was placed on a washed, dust-free microslide and dried naturally. These preparation steps were followed for the two other MBA

samples. Then these dried sediment samples were exposed under the laser with the wavelength of 532 nm, the intensity of 0.1%. All the Raman spectra records were drawn by Renishaw in Via.

3. Theoretical methods

The ground-state geometry of 2-MBA, 3-MBA and 4-MBA were all optimized with density functional theory (DFT), using the B3PW91 functional, 6-31G(d) basis set for C, H, O and S atoms and the LANL2DZ basis set for Ag4 atoms (Figure 1). All models have almost little imaginary frequency on these optimizations. The normal Raman scattering (NRS) spectra calculations indicate the same features and infrastructure in the ground state geometry optimization. All calculations were performed use the Gaussian 09 package for optimization.

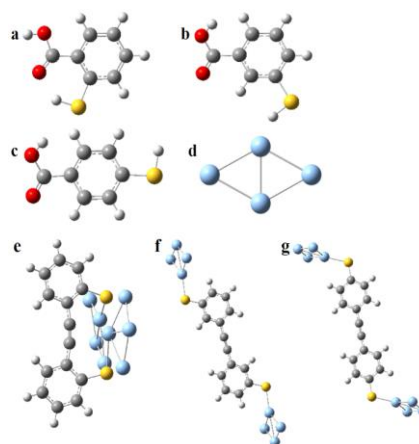


Figure 1: Optimized structures: a. 2-MBA, b. 3-MBA, c. 4-MBA, d. Ag₄ atoms, e. Ag 2-MBA, f. Ag 3-MBA, g. Ag 4-MBA.

4. Results and discussion

First, the absorption spectra of 2-MBA, silver sol and 2-MBA in silver sol were experimentally measured in the range of 200–400 nm (see Figure 2). It can be seen from Figure 2 that the absorption peak at around 257 nm in the UV spectra is the absorption peak of 2-MBA itself (black line), and it seems to be similar to the peaks of the 2-MBA with silver sol solution (blue line) and the pure 2-MBA solution (black line) at around 200 nm, respectively. In Figure 2, the obvious peaks (shown in the black and blue lines) appear at around 225 nm and 250 nm for 2-MBA, but there are no similar peaks for the silver sol solution. This indicates that resonance oscillation was not taking place between these two species upon photoexcitation due to their different optical energy levels. Significantly, a weak absorption peak is found at around 203 nm and 205 nm (1.24 eV) for 2-MBA in silver sol (see the blue line in Figure 2). This suggests the formation of a new compound which is likely to be a 2-MBA with silver sol complex caused by the interactions between 2-MBA and silver.

Second, we compared the 2-MBA NRS spectra from the experiment and the calculations, the specific vibration

spectrum peaks of some bonds are clearly labelled and indicate that these two spectra are well conformed (see Figure 3a). The experimental 2-MBA NRS and 2-MBA SERS spectra from 500 to 2850 cm^{-1} are shown in Figure 3d. Some differences are notable; for example, the NRS spectra (black and red lines) shows two peaks at around 805.32 cm^{-1} and 2512.63 cm^{-1} , but similar peaks have not appeared in the SERS spectra. By analysis of frequencies, it is likely that the in-plane bending and stretch vibrations of the S–H bond may cause the appearance of the peaks at around 804 cm^{-1} and 2500 cm^{-1} . So, it suggests that the S–H bond was disrupted, and the formation of S...Ag was generated [29]. In Figure 3d we also find there are two new peaks appeared at 2141.30 cm^{-1} and 2242.27 cm^{-1} in the SERS spectra, in comparison with the NRS spectra. Therefore, we can speculate that some specific new bonds have formed. In order to more accurately confirm the appearance of the new spectra peaks, the 2-MBA SERS and pure Ag sol NRS spectra are displayed in Figure 3c, there are no similar peaks at around 2000 to 2250 cm^{-1} in the pure Ag sol NRS spectra. Therefore, it is sufficiently proven that the emergence of the new peaks is probably owing to a particular reaction between 2-MBA and silver atoms on the surface due to the adsorption of 2-MBA on the silver atoms surface.

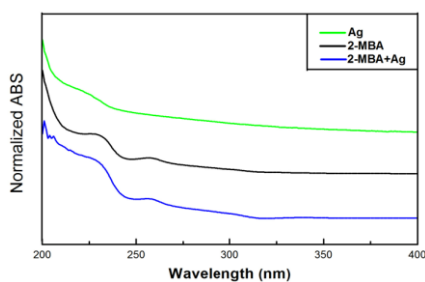


Figure 2: Absorption spectra of Ag sol (green line), 2-MBA (black line) and 2-MBA with Ag sol (blue line) from 200 to 400 nm.

According to the structure of the material and the interior specific chemical elements that were studied, and combining with the position of the new peaks (which can be directly deduced as the bond of $\text{C}\equiv\text{C}$), the final product is thiophenol acetylene (TPA). On the basis of this bold speculation, we attempted to simulate the structure of the ortho position TPA with Ag sol in the same conditions as 2-MBA Ag (Figure 1e) in Figure 1. Then we compared the SERS spectrum of the 2-MBA in the different conditions (experiment and calculation respectively) as shown in Figure 3b, and the specific vibration spectra bonds are also marked in the spectrum. However, in Figure 3d we find that the SERS spectrum in the experiment displays some similar peaks appearing in the NRS spectrum. This is because that the chemical reaction took place partly from silver sol with 2-MBA. Therefore, the 2-MBA has happened the reaction with silver sol and 2-MBA without reaction with silver sol is all present in the laser spot. In other words, the chemical bonds of the mixture that were not fully involved in the surface plasmon-catalysed reaction, as shown in the Figure 3d are the SERS spectrum (purple line) and NRS

spectrum (black line) from the experiment. These peaks do not contain the silver sol peaks (Figure 3c green line).

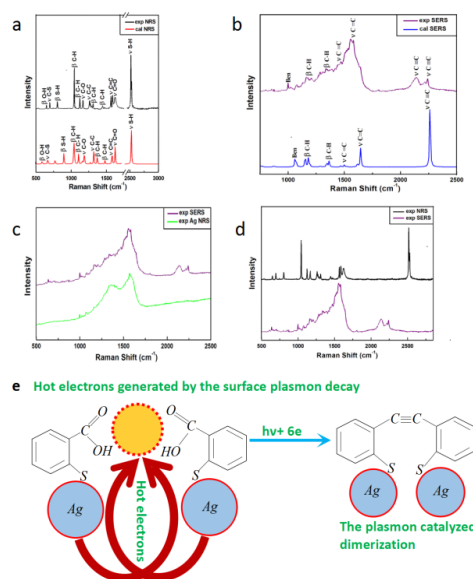


Figure 3: 2-MBA: a. The experimental (black line) and calculated (red line) NRS spectra, from 500 to 3000 cm^{-1} (β and ν indicate the in-plane bending and the stretching modes, respectively); b. The experimental (purple line) and calculated (blue line) SERS spectra, from 750 to 2500 cm^{-1} (β and ν indicate the in-plane bending and the stretching modes, respectively); c. The 2-MBA SERS spectrum (purple line) and Ag sol NRS spectrum (green line) from the experiment, from 500 to 2500 cm^{-1} ; d. The SERS spectrum (purple line) and NRS spectrum (black line) from the experiment, from 500 to 2850 cm^{-1} ; e. The plasmon-catalysed reaction of 2-MBA.

The mechanism for the surface plasmon-catalysed reaction of the 2-MBA converted to TPA can be seen in Figure 3e. The required $6e^-$ are proposed to be “hot electrons” arising from the surface plasmon decay. It is well known that the light quanta stored in the plasmons can be re-emitted as light partially, but a few of the plasmons can also decay into the two charge carriers, an electron and a “hole” [30]. After much research it was confirmed that the “hot electrons” can be created through the plasmons decay that can have high kinetic energy, which can presumably impel the surface plasmon-catalysed reaction. However, herein this reaction, we daringly thought that TPA was generated and that the $-\text{COOH}$ bond disappeared in the molecular structure of TPA through the observation of the spectrum of the final product, and so it is necessary to give a reasonable explanation. According to research of the basic chemical properties, the structure characteristics of an alkyne is that: two carbon atoms of the $\text{C}\equiv\text{C}$ bond exist in the sp hybridization, leaving two mutual perpendicular p orbitals with one electron for each carbon atom. An alkyne has a better ability to obtain electrons due to the strong electronegativity, so the electron cloud distribution of the benzene ring was influenced, and the electronegativity was also enhanced to a certain extent. Therefore, it is obvious to investigate the normal Raman relative intensity of the $\text{C}=\text{C}$ bond of the benzene ring which was strongly reinforced in Figure 3d (purple line) at around 1583.30 cm^{-1} and still further implies the generation of the new formation of an alkyne.

In Figure 4d and Figure 5d we can also find that the in-plane bending and stretching vibration of the S–H bond have disappeared. Combined with the above analysis, the results indicate that 3-MBA and 4-MBA are both adsorbed on the acid so that the position of the substituent group could change the intensity of the SERS signal.

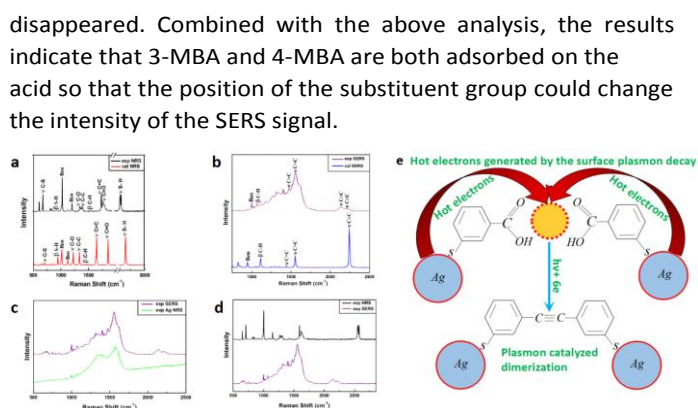


Figure 4: 3-MBA: a. The experimental (black line) and calculated (red line) NRS spectra, from 500 to 3000 cm^{-1} (β and ν indicate the in-plane bending and the stretching modes, respectively); b. The experimental (purple line) and calculated (blue line) SERS spectra, from 750 to 2500 cm^{-1} (β and ν indicate the in-plane bending and the stretching modes, respectively); c. The 3-MBA SERS spectrum (purple line) and Ag sol NRS spectrum (green line) from the experiment, from 500 to 2500 cm^{-1} ; d. The SERS spectrum (purple line) and NRS spectrum (black line) from the experiment, from 500 to 2850 cm^{-1} ; e. The plasmon-catalyzed reaction of 3-MBA.

Table 1: The frequency of the three MBAs in the NRS and SERS spectra (β and ν indicate the in-plane bending and stretching modes, respectively).

	2-MBA		3-MBA		4-MBA	
	NRS	SERS	NRS	SERS	NRS	SERS
S–H	2512.63 (ν)		2567.35 (ν)		2566.61 (ν)	
	805.32 (β)		915.43 (β)		807.02 (β)	
C=O	1623.40 (ν)		1622.87 (ν)		1622.77 (ν)	
C–O	1164.89 (ν)		1263.83 (ν)		1290.85 (ν)	
C=C	1584.57 (ν)	1583.30 (ν)	1595.21 (ν)	1560.62 (ν)	1589.57 (ν)	1575.98 (ν)
		1473.19 (ν)		1476.85 (ν)		1435.15 (ν)
	1446.80 (β)		1423.94 (β)	1401.13 (β)		
C–H	1313.83 (β)	1340.04 (β)				
	1120.21 (β)	1207.25 (β)	1147.34 (β)		1184.89 (β)	1180.55 (β)
	1043.09 (β)		1003.72 (β)			
C–C	1264.36 (ν)		1307.98 (ν)			
C–S	700.53 (ν)		710.64 (ν)		1091.70 (ν)	
C≡C		2242.27 (ν)		2219.38 (ν)		2335.68 (ν)
		2141.30 (ν)		2141.30 (ν)		2138.17 (ν)

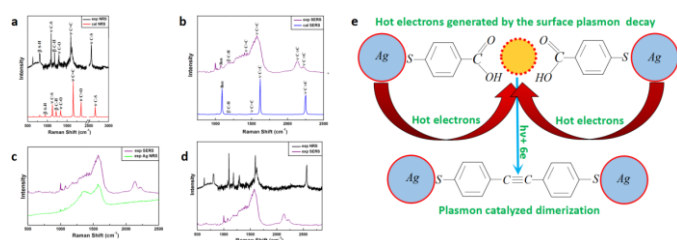


Figure 5: 4-MBA: a. The experimental (black line) and calculated (red line) NRS spectra, from 500 to 3000 cm⁻¹ (β and ν indicate the in-plane bending and the stretching modes, respectively); b. The experimental (purple line) and calculated (blue line) SERS spectra, from 750 to 2500 cm⁻¹ (β and ν indicate the in-plane bending and the stretching modes, respectively); c. The 4-MBA SERS spectrum (purple line) and Ag sol NRS spectrum (green line) from the experiment, from 500 to 2500 cm⁻¹; d. The SERS spectrum (purple line) and NRS spectrum (black line) from the experiment, from 500 to 2850 cm⁻¹; e. The plasmon-catalysed reaction of 4-MBA.

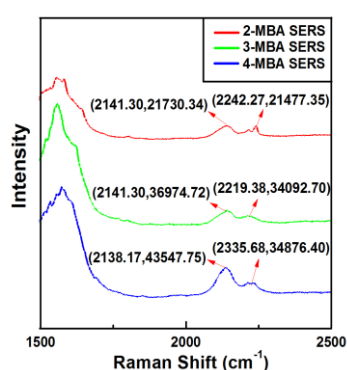


Figure 6: The SERS spectra of 2-MBA (red line), 3-MBA (green line) and 4-MBA (blue line) from 1500 to 2500 cm⁻¹, with detailed intensity marked respectively.

5. Conclusions

Silver sol was mixed with three MBA sample solutions, and placed respectively on the surface of dust-free slides and naturally dried. Under laser exposure, the surface plasmon-catalysed reaction was observed in the SERS spectra after the MBAs changed into TPA. Therefore, we could estimate the chemical composition of the final product from the comparison of NRS and SERS spectra. Therefore, this provides a simple and efficient method for monitoring the surface plasmon-catalysed reaction. The investigation not only enabled us to develop a new way to prepare thiophenol acetylene, but—~~it~~ also opened up a new direction for the research of substituent effect on the surface plasmon-catalysed reaction.

Acknowledgements

This work was financially supported by the National Natural Science Foundation of China (Grant No. 11274149, 11304135 and 11544015), the Shenyang Natural Science Foundation of China (F15-199-1-04), Liaoning Provincial Department of Education Project (Grant No. L2015200) and the Natural Science Foundation of Liaoning Province (Grant No. 201602345 and 201601095)

References

- [1] J. Lazarević, S. Uskoković-Marković, M. Jelikić-Stankov, M. Radonjić, D. Tanasković, N. Lazarević and Z. V. Popović, *Spectrochimica acta. Part A, Molecular and biomolecular spectroscopy*, 126 (2014) 301.
- [2] M. Alberto, D. Z. Mirella, T. Matteo and Z. Giuseppe, *J. Phys. Chem. B*, 112 (2008) 1619.
- [3] Y. Ma, K. Promthaveepong, and N. Li, *ACS Sens.*, 2 (2017) 135.
- [4] S. Sarkar, M. Pradhan, A. K. Sinha, M. Basu and T. PalThe, *J. Phys. Chem. Lett.*, 1 (2009) 439.
- [5] Y. Wang, B. Yan and L. Chen, *Chem. Rev.*, 113 (2012) 1391.
- [6] Y. Wang, W. Ji, Z. Yu, R. Li, X. Wang, W. Song, W. Ruan, B. Zhao and Y. Ozaki, *Phys. Chem. Chem. Phys.* 16 (2014) 3153.
- [7] C. Wang, X. Wu, P. Dong, J. Chen and R. Xiao, *Biosens. Bioelectron.*, 86 (2016) 944.
- [8] S. S. Sinha, S. Jones, A. Pramanik and P. C. Ray, *Acc. Chem. Res.*, 49 (2016) 2725.
- [9] C. Wei, M. M. Xu, C. W. Fang, Q. Jin, Y. X. Yuan and J. L. Yao, *Spectrochim. Acta A*, 175 (2017) 262.
- [10] W. Wei and Q. Huang, *Spectrochim. Acta A*, 179 (2017) 211.
- [11] H. Li, J. Jiang, Z. Wang, X. Wang, X. Liu, Y. Yan and C. Li, *J. Colloid Interface Sci.*, 501 (2017) 86.
- [12] H. Wu, H. Wanga and G. Li, *Analyst*, 142 (2017) 326.
- [13] A. Raj, Y. S. Mary, C. Y. Panicker, H. T. Varghese and K. Raju, *Spectrochim. Acta A*, 113 (2013) 28.
- [14] M. J. Tan, Z. Y. Hong, M. H. Chang, C. C. Liu, H. F. Cheng, X. J. Loh, C. H. Chen, C. D. Liao and K. V. Kong, *Biosens. Bioelectron.*, 96 (2017) 167.
- [15] M. Chen, W. Luo, Z. Zhang, F. Zhu, S. Liao, H. Yang and X. Chen, *Talanta*, 171 (2017) 152.
- [16] C. R. Forbes, S. K. Sinha, H. K. Ganguly, S. Bai, G. P. A. Yap, S. Patel, and N. J. Zondlo, *J. Am. Chem. Soc.*, 139 (2017) 1842.
- [17] G. D. Stynes, T. R. Gengenbach, G. K. Kiroff, W. A. Kirkland and M. A. Morrison, *J. Biomed. Mater. Res. A*, 105 (2017) 1940.
- [18] M. C. Rodríguez González, P. Carro, E. Pensa, C. Vericat, R. Salvarezza and A. Hernández Creus, *ChemPhysChem*, 18 (2017) 804.
- [19] R. Sahraei and M. Ghaemy, *Carbohydr. Polym.*, 157 (2017) 823.
- [20] L. Y. Jiang, X. S. Li, A. J. Wang, H. Huang and J. J. Feng, *J. Colloid Interface Sci.*, 498 (2017) 128.
- [21] T. Lahtinen, E. Hulkko, K. Sokołowska, T. R. Tero, V. Saarnio, J. Lindgren, M. Pettersson, H. Häkkinen and L. Lehtovaara, *Nanoscale*, 8 (2016) 18665.
- [22] Y. Levi-Kalisman, P. D. Jadzinsky, N. Kalisman, H. Tsunoyama, T. Tsukuda, D. A. Bushnell and R. D. Kornberg, *J. Am. Chem. Soc.*, 133 (2011) 2976.
- [23] S. K. Bhunia, L. Zeiri, J. Manna, S. Nandi and R. Jelinek, *ACS APPL MATER INTER*, 8 (2016) 25637.
- [24] S. G. Ilchenko, R. A. Lymarenko. And V. B. Taranenko, *Nanoscale Res. Lett.*, 12 (2017) 295.
- [25] M. L. Brongersma, N. J. Halas and P. Nordlander, *Nat. Nanotechnol.*, 10 (2015) 25.
- [26] Y. Shiraishi, N. Yasumoto, J. Imai and H. Sakamoto, S. Tanaka, S. Ichikawa, B. Ohtani and T. Hirai, *Nanoscale*, 9 (2017) 8349.
- [27] I. Chakraborty, A. Som, T. Adit Maark, B. Mondal, D. Sarkar and T. Pradeep, *J. Phys. Chem.*, 120 (2016) 15471.
- [28] P. Jia, J. Chang, J. Wang, P. Zhang, B. Cao, Y. Geng, X. Wang and K. Pan, *Chem-Asian J.*, 11 (2016) 86.
- [29] W. H. Liu, R. H. Yuan, Y. J. Teng, Y. P. Qin, Z. F. Pan and C. A. Ma, *Spectrosc. Spect. Anal.*, 33 (2013) 2433.
- [30] M. Sun and H. Xu, *Small*, 8 (2012) 2777.